Available online at www.sciencedirect.com
SCIENCE DIRECT®
Journal of Chromatography B, 798 (2003) 265–274
JOURNAL OF CHROMATOGRAPHY B
www.elsevier.com/locate/chromb

Metabolism of verapamil: 24 new phase I and phase II metabolites identified in cell cultures of rat hepatocytes by liquid chromatography–tandem mass spectrometry☆

M. Walles[a], T. Thum[b], K. Levsen[a], J. Borlak[b,*]

[a] *Department of Analytical Chemistry, Fraunhofer Institute of Toxicology and Experimental Medicine, 30625 Hannover, Germany*
[b] *Department of Drug Research and Medical Biotechnology, Fraunhofer Institute of Toxicology and Experimental Medicine, Nikolai-Fuchs Str. 1, 30625 Hannover, Germany*

Received 19 February 2003; received in revised form 15 July 2003; accepted 25 September 2003

Abstract

Verapamil is a widely prescribed calcium antagonist, but suffers from extensive first pass metabolism. Despite its frequent use in drug metabolism a complete understanding of its metabolic pathway is still lacking. We thus investigated verapamil's metabolism in cultures of primary rat hepatocytes and isolated metabolites from cell culture media by solid phase extraction (SPE). In detail, we investigated their structure in multiple liquid chromatography–mass spectrometry (LC–MS^n) experiments and found 25 phase I and 14 phase II metabolites. We showed many metabolites to be produced by oxidative dealkylation, and several yet unknown metabolites were identified that stem from hydroxylation and dealkylation reactions. Furthermore, we identified an array of glucuronides and, additionally, a glucoside. Finally, we investigated the enantioselective biotransformation of verapamil and found preferential metabolism of the *S*-enantiomers. In conclusion, this illustrates again the true complexity of verapamil's disposition.

Keyword: Verapamil metabolites

1. Introduction

Verapamil is a commonly prescribed calcium antagonist with anti-anginal, anti-hypertensive and anti-arrythmic properties. The metabolites of verapamil found so far partly show pharmacological properties. Verapamil suffers from extensive first pass metabolism. It is therefore important to develop sample preparation and analysis techniques for screening verapamil metabolites in different biological matrices.

A variety of methods for analyzing verapamil metabolites have been published. Most methods apply liquid chromatography–tandem mass spectrometry (GC–MS) (usually after derivatization) to characterize the main metabolites of verapamil [1–3]. One disadvantage of GC–MS is that polar compounds cannot be analyzed without derivatization. Consequently, it is difficult to analyze phase II compounds like glucuronides with this method, although an identification of the norverapamil glucuronide after derivatization with GC–MS has been described [4]. This is the only glucuronide that has been reported so far.

Liquid chromatography coupled to an ion trap mass spectrometer with ESI source allows a direct identification of polar compounds like glucuronides without prior derivatization. An ion trap mass spectrometer with multi-stage MS capabilities (MS^n) as used in our study is particularly suited for the identification of unknown metabolic breakdown products.

A very sensitive method based on LC–MS^n with an ESI interface has been described recently to determine the main metabolites of verapamil in various biological matrices [5].

Here, we focused on the identification and structure elucidation of new, less abundant metabolites of verapamil. These include newly identified glucuronides and glucosides formed in cell cultures of primary rat hepatocytes. Finally, we also investigated enantioselective phase II metabolism.

☆ Supplementary data associated with this article can be found, in the online version, at doi:10.1016/j.jchromb.2003.09.058.

* Corresponding author. Tel.: +49-511-5350-559; fax: +49-511-5350-573.
E-mail address: borlak@item.fraunhofer.de (J. Borlak).

1570-0232/$ – see front matter © 2003 Elsevier B.V. All rights reserved.
doi:10.1016/j.jchromb.2003.09.058

Overall, this study aims to provide in-depth information on the true complexity of verapamil's metabolism.

2. Methods

2.1. Materials and chemicals

AcCN (Malinckrodt-Baker, Deventer, The Netherlands), MeOH (Malinckrodt-Baker, Deventer, The Netherlands), ammonium acetate (Merck, Darmstadt, Germany), acetic acid (Fluka, Buchs, Switzerland), Norverapamil (5-*N* (3, 4-dimethoxyphenethyl) amino-2-(3′,4′-dimethoxyphenyl)-2-isopropyl-valeronitrile) (Research Biochemicals International, Natick, MA, USA), racemic verapamil (5-*N*-(3,4-dimethoxyphenethyl)methylamino-2-(3′,4′-dimethoxyphenyl)-2-isopropylvaleronitrile) (Lot56H0925/Sigma–Aldrich, Steinheim, Germany), *S*-verapamil and *R*-verapamil (Sigma–Aldrich, Steinheim, Germany), β-glucuronidase (type H-1, 367500 U/g, Sigma–Aldrich, Steinheim, Germany). The 2, 3, 6, 15, 16, 19 verapamil-d_6 and the metabolites D-715 and D-703 were a kind gift of Prof. W.L. Nelson (University of Washington, Seattle, USA).

2.2. Animals

All animal procedures described in this report were approved by the ethical committee of the city of Hanover and the investigation conforms to the *Guide for the Care and Use of Laboratory Animals* published by the US National Institutes of Health (NIH Publication No. 85-23, revised 1996). Male Sprague–Dawley rats weighing about 200 g were obtained from Charles River (Sulzfeld, Germany). Food and water was given ad libitum. Anesthesia: rats were anesthetized with 0.1 ml of Ketamin per 100 g body weight and 0.05 ml of xylazin-hydrochloride per 100 g body weight. In addition, 2.000 international units of Heparin were given intraperitoneally prior to surgery.

2.3. Isolation and cultivation of hepatocytes

A modified method originally described by Seglen [6] was used to isolate hepatocytes. In brief, the portal vein was cannulated after midline incision, and the liver was first perfused in situ with 100 ml calcium-free Krebs Ringer buffer (KRB) for 10 min, then with 100 ml KRB and EDTA (1 mmol/l). Next, the liver was perfused for 8–10 min with KRB supplemented with Collagenase type IV (Worthington, Freehold, USA) and 0.5 mM calcium chloride (Sigma, Deisenhofen, Germany). After perfusion, the liver capsule was gently removed and the dissolved parenchymal tissue filtrated through a nylon mesh (pore size 100 μm) and washed two times with the washing buffer (1000 ml Hanks balanced salt solution (PAA, Germany) supplemented with 2.4 g hydroxy-ethyl-piperazine-ethane-sulfonic acid (HEPES; Sigma, Germany) and 2 g bovine serum albumin (Sigma, Deisenhofen, Germany) followed by centrifugation at 4 °C and 1200 rpm for 5 min. The cell pellet was resuspended in William's E medium (Biochrom, Berlin, Germany) supplemented with 5% fetal calf serum (FCS; Biochrom, Germany), 9.6 μg/ml prednisolone, 0.014 μg/ml glucagon (Novo, Germany), 0.16 U/ml insulin (Hoechst, Germany), 200 U/ml penicillin and 200 U/ml streptomycin (GIBCO, Germany). Hepatocytes were counted in a hemocytometer (Neubauer-chamber) in the presence of 0.04% trypan-blue solution. Two million hepatocytes per dish were cultured on a collagen type I layer, and after 24 h in culture non-adherent cells were removed and the second collagen layer was applied as originally described by Dunn et al. [7]. Hepatocytes were allowed to recover for 48 h and were then used for further experiments.

Verapamil (2 μM), *R*-verapamil (2 μM), *S*-verapamil (2 μM) or verapamil-d_6 (2 μM) were added to hepatocyte cultures for 24 h and culture supernatant was removed and frozen (−80 °C) subsequently for further studies.

2.4. Sample preparation

The proteins of the culture media were precipitated with 6 ml of methanol and removed by centrifugation (centrifuge from Sigma, Osterode, Germany, type 1–15, diameter of rotor = 16.4 cm) at 3000 rpm for 5 min. The resultant supernatant was evaporated to dryness using a gentle stream of nitrogen.

In assays with verapamil antipodes, the cell culture media was split in a ratio of 2:1. First, 50 μl of a gallopamil standard solution (1 μg/ml) were added to both solutions as an internal standard. The glucuronides were cleaved with β-glucuronidase (approximately 1850 units) and dissolved in 0.01 M ammonium acetate/acetic acid buffer at a pH of 4.5 for 12 h at 37 °C. After incubation, the proteins were removed as described above.

2.5. Extraction and LC–MS^n analysis

Verapamil and its basic metabolites were analyzed by solid phase extraction (SPE) followed by high-performance liquid chromatography–mass spectrometry.

For SPE a lipophilic cartridge (RP8 Select B, Merck, Germany) was used which was conditioned with 4 ml methanol followed by equilibration with 4 ml water. The sample was loaded onto the cartridge without any organic solvent and washed with 5% methanol to separate any sample matrix. Verapamil and its basic metabolites were eluted with 2 ml methanol. The eluent was evaporated to dryness and reconstituted in 200 μl of acetonitrile/ammonium acetate (0.01 M, pH 6.0, 50/50, v/v). Aliquots of 20 μl were injected onto the LC–MS system.

LC–MS analyses were done on a Waters (Milford, MA, USA) LC instrument (pumps 590) coupled to an ion trap mass spectrometer (Esquire from Bruker Daltonik, Bremen, Germany) that operated under positive ion electrospray (ESI)

Table 1
Main fragmentation of conjugated and non-conjugated metabolites of verapamil

No.	Phase I[a]			Phase II		Substituents										Phase I	Phase II	Cleavages (m/z)[b]						Neutral losses, fragments and other low abundant (<5%), non significant ions
	R_t (min)	Abundance[c] (%)	S/R	R_t (min)	S/R	R1	R2	R3	R4	R5	R6	R7	R8	R9	R10	$[M+H]^+$ or m/z	$[M+H]^+$	A_1[d]	A_2	B_1[d]	B_2	B_3[d]	C	
1 Vera[e,f,g]	49.8	100	3.6	15.3	3.2	OCH_3	OCH_3	OCH_3	OCH_3	CH_3	H	C_3H_7	H	H	H	455	631	150	303	165	–	260	–	216, 238, 262, 337
2 Norv.[h,g]	47.1	180	–	16.8[i]	–	OCH_3	OCH_3	OCH_3	OCH_3	H	H	C_3H_7	H	H	H	441	617	151	289	165	–	260	398	247
3 D620[e,g,j]	25.6	8.0	1.4	4.5	1.5	–	–	OCH_3	OCH_3	H	–	C_3H_7	H	H	H	277	453	–	–	–	–	260	234	–
4 D717[e,j]	28.6	9.5	1.4	5.7	1.3	–	–	OCH_3	OH	CH_3	–	C_3H_7	H	H	H	277	453	–	–	–	–	246	234	218
5 D617[h,g,j]	30.0	122	1.5	15.2[i]	1.3	–	–	OCH_3	OCH_3	CH_3	–	C_3H_7	H	H	H	291	453	–	–	–	–	260	248	333, 369, 417, 435
6	21.9	0.02	1.3	–	–	–	–	OCH_3	OH	H	–	C_3H_7	H	H	H	263	–	–	–	–	–	246	221	204, 128, 198, 229
7 D702[e,f,g]	43.2	230[k]	–	7.1	2.0	OH	OCH_3	OCH_3	OCH_3	CH_3	H	C_3H_7	H	H	H	441	617	–	303	151	291	260	248	–
8 D703[e,f,g]	44.0	230[k]	1.2	8.80	0.7	OCH_3	OCH_3	OCH_3	OH	CH_3	H	C_3H_7	H	H	H	441	617	151	289	165	–	246	–	133, 372
9[e,g]	45.0	230[k]	–	10.1	1.0	OCH_3	OH	OCH_3	OCH_3	CH_3	H	C_3H_7	H	H	H	441	617	–	303	151	291	260	248	187, 373
10[g]	38.7	12	–	10.3	–	OH	OCH_3	OCH_3	OH	CH_3	H	C_3H_7	H	H	H	427	603		289	151	277	246	384	–
11[e,f,g]	42.0	200[l]	1.6[l]	7.4	1.9	OH	OCH_3	OCH_3	OCH_3	H	H	C_3H_7	H	H	H	427	603	–	–	151	277	260	384	–
12 D715[e,f,g]	42.9	200[l]	1.6[l]	9.0	1.1	OCH_3	OCH_3	OCH_3	OH	H	H	C_3H_7	H	H	H	427	603	150	275	165	–	(246)	384	233, 306
13	36.1	0.4	–	–	–	OCH_3	OCH_3	OH	OH	H	H	C_3H_7	H	H	H	413	–	150	261	165	–	–	–	135, 221, 367, 377, 395 ($-H_2O$)
14[e,m]	37.1	0.5	–	–	–	OH	OCH_3	OCH_3	OH	H	H	C_3H_7	H	H	H	413	–	–	275	151	263	246	370	206, 234, 395
15[m,f]	39.3	1.5	4.6	–	–	OCH_3	OCH_3	OCH_3	OCH_3	CH_3	OH	C_3H_7	H	H	H	471	–	–	303	181	291	260	–	234, 248, 453 ($-H_2O$)
16[e]	39.0	1.4	1.4	11.1	1.2	OCH_3	OCH_3	OCH_3	OCH_3	CH_3	OH	C_3H_7	H	H	H	471	647	–	(303)	181	291	260	248	453 ($-H_2O$)
17[e]	42.8	3	1.4	11.2	1.5	OCH_3	OCH_3	OCH_3	OCH_3	H	OH	C_3H_7	H	H	H	457	633	–	289	181	277	260	414	235, 399, 439 ($-H_2O$)
18[e,f,g]	34.3	1.2	1.9	11.3	–	OCH_3	OCH_3	OCH_3	OCH_3	CH_3	H	C_3H_6OH	H	H	H	471	647	150	319	165	–	–	413	261, 453 ($-H_2O$)
19	41.5	0.8	S[n]	–	–	OCH_3	OCH_3	OCH_3	OH	CH_3	H	C_3H_6OH	H	H	H	457	–	150	–	165	–		398	220, 194, 247, 284, 399, 439 ($-H_2O$)
20[m]	31.9	1.2	1.9	–	–	OCH_3	OCH_3	OCH_3	OCH_3	CH_3	H	C_3H_7	H	OH	H	471	–	150	319	165	–	276	–	191, 249, 440
21[e,m]	36.6	0.9	3.4	–	–	OCH_3	OCH_3	OCH_3	OCH_3	CH_3	H	C_3H_7	H	H	OH	471	–	(151)	319	165	–	276		234, 206, 258, 259
22	32.1	2.5	2.2	–	–	OCH_3	OCH_3	OCH_3	OCH_3	H	H	C_3H_7	OH	H	H	457	–	150	305	165	–	276	–	247, 206, 220, 439 ($-H_2O$)
23[m]	35.4	0.9	0.6	–	–	OCH_3	OCH_3	OCH_3	OCH_3	H	H	C_3H_7	H	H	OH	457	–	151	305	165	–	276	–	135, 206, 307, 384, 440
24[f]	42.0	1.2	–	–	–	OCH_3	OCH_3	OCH_3	OCH_3	CH_2OH	H	C_3H_7	H	H	H	471	–	151	–	165	–	260	–	453 ($-H_2O$)
25[h,f]	–[i]	1.8	–	–	–	OCH_3	OCH_3	OCH_3	OCH_3	CHO	H	C_3H_7	H	H	H	469	–	151	–	165	–	260	–	441 (–CO)

m/z values in parentheses: low abundance fragments (2–4% relative abundance).

[a] Phase I metabolites after cleavage with β-glucuronidase.

[b] Cleavages: reported m/z values are from MS^3 of the $[M+H-176]+$ ions of the phase II metabolites and of the MS^2 spectra of the $[M+H]^+$ ions of the phase I metabolites.

[c] Relative peak area of the phase I metabolites compared to verapamil.

[d] Cleavage is accompanied by charge migration.

[e] These metabolites have been identified from one single pool of several rats: pool ca. 30 ml medium.

[f] Structures have been additionally confirmed by incubations with d_6-labelled verapamil: pool ca. 20 ml.

[g] Metabolite appears also in non-conjugated form.

[h] These metabolites have been identified from the pool of a different rat: pool ca. 30 ml; all other metabolites not labelled a or b were detected in both pools.

[i] Metabolite has been recorded under different chromatographic conditions.

[j] Phenylethyl moiety lost.

[k] Sum of the abundances of the non-conjugated metabolite 7, 8 and 9.

[l] Sum of the abundances of the non-conjugated metabolite 11 and 12.

[m] Position of the hydroxyl group could not be located unambiguously.

[n] Only the *S*-enantiomer has been detected.

conditions in the full scan, MS^2 and, in some instances, in the MS^3 and MS^4-mode. The nebulizer pressure was set to 40 psi and the dry gas temperature to 350 °C, while +3 kV were applied to the nebulizing capillary. Full mass spectra were acquired by scanning the mass range of *m/z* 100–700. CID spectra (collision gas: helium) were obtained from the protonated molecules $[M + H]^+$. HPLC analysis was carried out with a gradient elution of ammonium acetate buffer (0.01 M, pH 6.0) and acetonitrile using a flow of 0.2 ml/min. The gradient starts with 25% acetonitrile, increasing to 50% within the first 15 min and to 75% acetonitrile from 15 to 30 min. From 30 to 55 min the acetonitrile content remains constant and decreases to 25% from 55 to 60 min. Separation of verapamil and its metabolites was achieved on a 250 mm × 2 mm RP Select B column with a particle size of 4 μm (Merck, Darmstadt, Germany).

For identification of conjugates of metabolites 2 and 5 different chromatographic conditions were used (index h in Table 1): A RP8 Select B column was used for separation (250 mm × 4 mm, 5 μm). HPLC separation was carried out with a solvent composition of acetonitrile and water using a flow rate of 0.6 ml/min. An accurate splitter was used to split the flow 1:3 before introduction into MS.

The gradient started with 25% acetonitrile and the acetonitrile was increased to 80% within the first 30 min. Then the acetonitrile content was kept constant to 80% up to 60 min before it decreased again to 25%.

Identification of metabolites was done by collision-induced dissociation (CID) experiments in multiple LC–MS/MS (MS^2), LC–MS^3 and LC–MS^4 experiments.

To distinguish the metabolites from artefacts blank cell culture media (William's E medium (Biochrom, Berlin, Germany)) supplemented with 5% fetal calf serum (Biochrom, Germany), 9.6 μg/ml prednisolone, 0.014 μg/ml glucagon (Novo, Germany), 0.16 U/ml insulin (Hoechst, Germany), 200 U/ml penicillin and 200 U/ml streptomycin (GIBCO, Germany) and blank culture media (without cells) spiked with verapamil was incubated, extracted and analyzed under the same conditions as described above.

2.6. Recovery

For recovery experiments (done in quadruplicates), a blank cell culture supernatant solution was spiked with verapamil and norverapamil in a concentration range from 1 ng/ml to 1 μg/ml followed by solid phase extraction as described above. The resulting eluent was reduced in volume to 200 μl. Measurement of these extracts was done as described above. Recoveries were determined by comparing the peak areas to those of a standard solution injection. Recoveries of 85 ± 4 and 81 ± 5% for verapamil and norverapamil, respectively, were observed.

2.7. Quantification

The abundances in Table 1 were calculated by comparing the peak ratios of the metabolites relative to that of verapamil (100%), see Table 1. They give only semi quantitative information on the concentrations of the metabolites relative to that of verapamil, as the ionization efficiency of the various metabolites under ESI may vary.

The *S*/*R* ratio of the enantiomers was calculated by quantification with the internal standard. *S*/*R* ratios were considered as significant when the differences between both enantiomers were ≥4 time the relative standard deviation. Only metabolites with a s/n of six times the R.S.D. were quantified and are listed in Table 1.

3. Results

3.1. Structure elucidation of the metabolites by LC–MS^n

The structures of the metabolites were investigated by comparing their MS fragmentation pattern (see Table 1) with that of verapamil. In a first step, the mass of the quasi molecular ion of each metabolite was compared with that of verapamil to provide a first indication of the structure of the metabolite; in a second step, this proposed structure was confirmed by studying the collision-induced fragments (only ions with a relative intensity of >5% are discussed). Although only a mass spectrometer (ion trap) with unit mass resolution for both the quasi molecular and the fragments ions was available, the elemental composition of the fragments was unambiguous (with two exceptions discussed below). However, mass spectrometry alone is not always sufficient for identifying the site of a biotransformation (i.e. the site of a hydroxylation or glucuronidation). Here, nuclear magnetic resonance (NMR) would be the technique of choice; however, this technique failed due to the low amounts of metabolites observed in the cell cultures. Some metabolites formed in rat heart tissue have been published recently by us [8].

3.1.1. Collision-induced dissociation of protonated verapamil and its phase I metabolites

The collision-induced dissociation of protonated verapamil and its metabolites proceeds mainly via some well-defined fragmentation pathways as illustrated in Fig. 1 (where it is assumed that the initial protonation occurs at the nitrogen):

(a) Cleavage of the C–C-bond in the α-position to the nitrogen of the substituted phenylethyl moiety and charge migration (in some instances accompanied by hydrogen transfer) (route A_1 in Fig. 1) leading to the fragment ion $[A_1]^+$ or cleavage of this bond with charge retention and hydrogen transfer to the eliminated neutral, i.e. a substituted toluene (route A_2 in Fig. 1) leading to the ion $[A_2 - H]^+$.
(b) Cleavage of the N–C bond of the substituted phenylethyl moiety, charge migration and elimination of a highly substituted phenylbutylamine as neutral (route B_1)

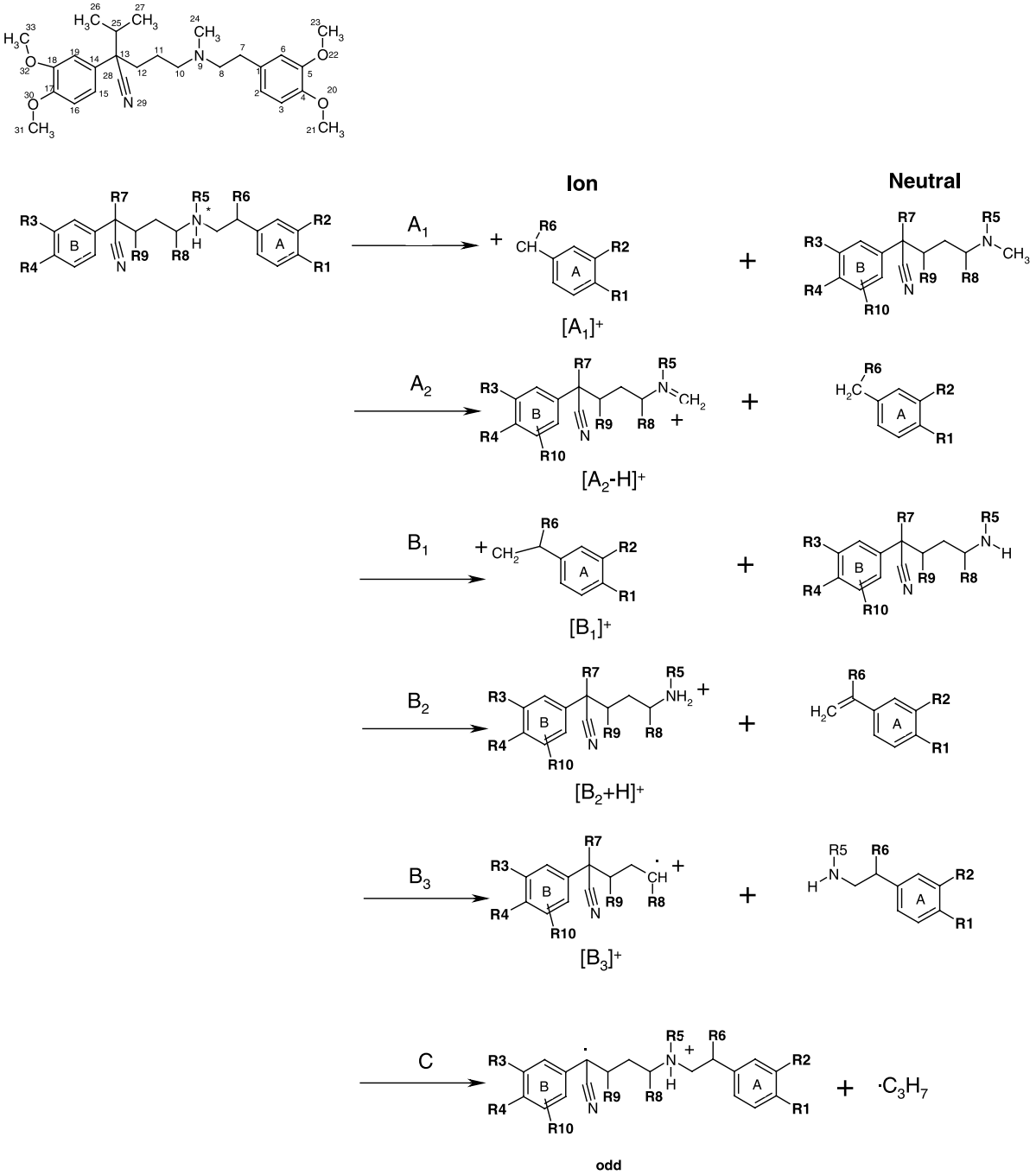

Fig. 1. Structure and main fragmentation pathways of verapamil and metabolites.

leading to the fragment ion $[B_1]^+$ or cleavage of this bond with charge retention and hydrogen transfer onto the nitrogen with elimination of a substituted styrene as neutral (route B_2 in Fig. 1) leading to the ion $[B_2 + H]^+$.

(c) Alternatively, also cleavage of the N–C bond on the highly substituted phenylbutyl moiety and elimination of substituted phenylethylamine as neutral may occur (B_3) leading to the fragment ion $[B_3]^+$ (Fig. 1).

(d) In addition, many metabolites show an abundant loss of water which (in conjunction with the observed shift of the *m/z* value of the protonated molecule by 16 Da) is characteristic of the presence of a hydroxyl group in the aliphatic moiety.

(e) Finally, loss of ammonia during the fragmentation proves the presence of a primary amine and loss of methylamine the presence of a secondary methylamine; loss of acetone is characteristic of a hydroxylation

of the isopropyl group, and loss of carbon monoxide shows the presence of a carbonyl group.

(f) In general, all fragmentation pathways discussed so far lead to thermochemically stable, even electron fragment ions by loss of an even electron neutral molecule (even electron rule).

(g) In contrast, loss of a propyl radical from the protonated molecule or a primary fragment ion (as observed with most metabolites) leads to an odd electron fragment ion (a process which is probably favored by the adjacent cyano group) (C in Fig. 1). Note, however, that a competing (thermodynamically more favorable) loss of a propene molecule is also observed in some instances.

(h) Other cleavages of the alkyl chains are observed less frequently. All these additional fragments are listed in the last column of Table 1.

It is of interest that the presence of a hydroxy group on the substituted phenylethyl moiety (independent of its location) influences the fragmentation of the protonated verapamil metabolites significantly: the fragmentation route B_2 is observed only if such a hydroxy group is present in the substituted phenylethyl part of the molecule, while lack of this group leads to the fragmentation channel A_1. In contrast, a hydroxy group on the highly substituted phenylbutylamine moiety apparently has no effect on the fragmentation.

Metabolic transformation of verapamil leads to characteristic changes in the masses (m/z values) of these fragment ions, which (together with the m/z value of the quasi molecular ion) allow the identification of the type and, to a large extent, also the position of the metabolic transformation, as shown below.

Using this approach, 24 phase I metabolites were identified as summarized in Table 1, which lists the m/z values of the main fragment ions of these metabolites. If the metabolite was also observed in the conjugated (usually glucuronidated) form, the fragment ions of the glucuronide are listed in Table 1 (except for verapamil). Note that the collision-induced loss of the glucuronic acid moiety (176 Da) from these conjugates leads to the protonated phase I metabolite. Thus, the MS^3 spectra of the $[M-176]^+$ ions of the glucuronides and the MS^2 spectra of the corresponding protonated phase I metabolites are almost identical.

In the following, the structure assignment of the 24 phase I metabolites, as based on their mass spectrometric fragmentation behavior, is only summarized (a detailed discussion of the mass spectrometric fragmentation is available upon request).

3.1.2. Verapamil and norverapamil

Most metabolites summarized in Table 1 can be rationalized to originate either from verapamil (**1**) or norverapamil (**2**), which are therefore discussed first (although the *N*-demethylation leading to (**2**) is not necessarily the first step). The protonated verapamil (**1**) fragments via route A_1 (with hydrogen transfer, $m/z = 150$), A_2 ($m/z = 303$), B_1 ($m/z = 165$) and B_3 ($m/z = 260$), see Fig. 1 and Table 1, while with norverapamil the fragmentation route C (m/z 398) is also observed. Oxidative *N*-demethylation of verapamil giving rise to norverapamil (**2**) is reflected by a mass shift of the ion $[A_2\text{-H}]^+$ by 14 Da. The fragments of both (**1**) and (**2**) were confirmed by comparison with synthetic reference compounds. Verapamil and norverapamil were also observed as glucuronides.

3.1.3. Metabolites formed by oxidative dealkylation and additional demethylation

The metabolites (**3**) (D-620), (**4**) (D717), (**5**) (D 617) and (**6**) are formed by oxidative dealkylation (loss of the substituted phenylethyl moiety) as shown by the m/z value of their quasi molecular ion and corroborated by their collision-induced fragments. While with (**3**) and (**6**) fragmentation route B_3 proceeds via loss of ammonia (leading to m/z 260 for (**3**) and $m/z = 246$ for (**6**)), consistent with a *N*-demethylation, loss of methylamine (leading to $m/z = 246$ for (**4**), but to $m/z = 260$ for (**5**)) is observed for (**4**) and (**5**), which consistent with a retention of the methyl group at the nitrogen. Instead *O*-demethylation must have occurred with (**4**), which is corroberated by the observed fragments $[B_3]^+$ at $m/z = 246$. Finally, (**6**) must have been formed by oxidative *N*-dealkylation, *N*-demethylation and *O*-demethylation as demonstrated not only by the precursor ion mass, but also by loss of ammonia ($m/z = 246$) and the mass shift of the fragment ion due the route C (loss of isopropene) (as compared to (**3**)) and the fragment at $m/z = 204$ (route D in Fig. 1). The observed loss of 31 from (4) and (6) indeed corresponds to loss of methylamine and not to the isobaric methoxy group as shown by hydrogen/deuterium exchange experiments [9].

The masses of the quasi molecular ions and their collision-induced dissociations thus allow an unambiguous structure elucidation of the metabolites (**3**)–(**6**) with one exception: Mass spectrometry does not permit to determine which of the two methoxy groups of (**4**) and (**6**) was demethylated. However, an HPLC/NMR/MS study of verapamil metabolites in human urine demonstrated that a demethylation of the methoxy group in trans position (bound to C_{17}) occurred for (**4**) [9], a result which can very likely be extended to the metabolites (**4**) and (**6**) observed in this study in hepatocytes of rats.

The metabolites (**3**)–(**5**) were also detected in the conjugated form, (**3**) and (**4**) as glucuronide, and (**5**) as glucoside.

3.1.4. Metabolites formed by oxidative O- and N-demethylation

The metabolites (**7**)–(**14**) are formed by oxidative demethylation, which can occur one or two times. In part, an additional *N*-demethylation is observed. Thus, some of these metabolites can be rationalized to originate from verapamil, i.e. (**7**)–(**10**), and others from norverapamil (**11**)–(**14**), even if *N*-demethylation is not necessarily the

first step. If *O*-demethylation of verapamil occurs once, a quasi molecular ion of $m/z = 441$ (14 Da lower than verapamil) is observed, and if this demethylation occurs twice, a quasi molecular ion at $m/z = 427$ (2×14 Da lower than verapamil) is found. *O*-demethylation can occur at ring A or B (see Fig. 1). The *m/z* value of the fragment formed via route A_2 reveals the position of the *O*-demethylation: if this value does not shift (as compared to verapamil) a methoxy group at ring A is demethylated, i.e. with (**7**) and (**9**), while a demethylation at ring B lowers this *m/z* value by 14 Da as observed with (**8**). In contrast just the opposite behavior is observed for ions formed via route B_1 leading to the substituted phenylethlyl ion $[B_1]^+$: demethylation at ring A lowers the *m/z* value of this ion by 14 Da, as compared to verapamil and observed for (**7**) and (**9**), while no mass shift is observed if demethylation occurs at ring B as in (**8**). A similar reasoning can be used to demonstrate that with the metabolite (**10**), one *O*-demethylation occurs at ring A and the other at ring B. Single and double *O*-demethylation is also observed for those metabolites derived from norverapamil, i.e. (**11**)–(**14**). If, for instance, *m/z* of the $[A_2\text{-H}]^+$ ion is shifted to lower values by 14 Da as compared to norverapamil, a single demethylation at ring B has occurred, i.e. with (**12**) and (**14**). If, however, this value is shifted by 2×14 Da, two demethylations at ring B have taken place, e.g. with (**13**). Similarly, the *m/z* value of the $[B_1]^+$ ion (when compared to norverapamil) reveals any demethylation at ring A, as with (**14**).

As mentioned above, the presence of a hydroxyl group at the substituted phenylethyl moiety (here the aromatic ring A) opens up a new decomposition channel, i.e. B_2, as observed with (**7**), (**9**)–(**11**) and (**14**). The occurrence of the ion $[B_2 + H]^+$ and its *m/z* value confirms the structure assignment of the *O*-demethylation products (**7**)–(**14**). This assignment is furthermore corroborated by the *m/z* value of the $[B_3]^+$ ion (shift by 14 Da if ring B is demethylated once, as with (**10**), (**12**) and (**14**)).

While the collision-induced fragments, together with the mass of the quasi molecular ion, not only enable us to determine the number of *O*-demethylations but also the position within the molecule (ring A or B), it is not possible to prove which of the two methyl groups at a given aromatic ring is demethylated using this technique. The above mentioned NMR study of verapamil metabolites in human urine revealed that in the case of metabolite (**12**), the trans methoxy group was demethylated again [9].

For metabolite (**8**) (D703) a reference compound was available the fragmentation of which further supported the above structure assignment. The metabolites (**7**)–(**14**) where also observed in the conjugated form.

3.1.5. Metabolites formed by hydroxylation

Within this study, 10 metabolites formed by hydroxylation were observed although with low abundance (i.e. (**15**)–(**24**)). This metabolic route has not been described previously for verapamil. The metabolites (**15**), (**16**), (**18**), (**20**) and (**21**) are formed by direct hydroxylation of verapamil, which leads to $m/z = 471$ for the quasi molecular ion, 16 Da higher than that of verapamil. Those derived from norverapamil (**17**), (**22**) and (**23**), form a quasi molecular ion of $m/z = 457$, 16 Da higher than that of norverapamil. If hydroxylation occurs at the substituted phenylethyl moiety, the *m/z* value of the fragment $[B_1]^+$ must be shifted by 16 Da when compared to both verapamil and norverapamil (as found with (**15**)–(**17**)), while the *m/z* value of this fragment is not shifted if hydroxylation occurs at the highly substituted phenylbutyl moiety of the molecule, i.e. with (**18**)–(**23**). In this case, *m/z* of the fragment $[B_3]^+$ (if observed) increases by 16 Da, while $[B_1]^+$ is not shifted, as is found with (**18**)–(**23**). Finally, as discussed above, hydroxylation at the substituted phenylethyl moiety triggers the additional fragmentation according to route B_2 in Fig. 1 as observed with (**15**)–(**17**). The *m/z* values of the $[B_2 + H]^+$ ions formed via this route confirm this conclusion.

What additional information on the position of the hydroxyl group is available from mass spectrometry? In general, a phenolic hydroxyl group in a protonated molecule is not lost as neutral water upon collision-induced dissociation (but, if at all, as hydroxyl radical), while an abundant loss of water is found with alcohols. Consistent with this observation, the protonated metabolites (**4**), (**6**)–(**14**), which after oxidative demethylation have one or two hydroxyl groups bound to the aromatic ring, do not undergo collision-induced loss of water, with one exception: The protonated metabolite (**13**) with two vicinal hydroxy groups shows an abundant loss of water.

In contrast, the protonated metabolites formed by hydroxylation, i.e. (**15**)–(**19**), (**22**) and (**24**), undergo in all but three instances collision-induced loss of water, strongly suggesting that the hydroxyl group is bound to an aliphatic carbon. Alternatively, the lack of water loss can be considered as a strong indication for a hydroxylation occurring at the aromatic ring, e.g. with the metabolites (**20**), (**21**) and (**23**).

Furthermore, and according to the above discussion, the hydroxyl group in (**15**)–(**17**) showing a loss of water must be bound to the aliphatic part of the substituted phenylethyl moiety, i.e. to C_7 or C_8. The *m/z* values of the $[A_2\text{-H}]^+$ ions, which comprise C_8 and are not shifted when compared to verapamil (**1**) or norverapamil (**2**), prove that the hydroxyl group must be bound to C_7 at least for (**15**) and (**17**) (the identification of (**16**) which shows similar *m/z* values as (**15**) is less safe. Note that hydroxylation at C_7 leads to a new chirality center so that (**15**) and (**16**) could be diastereomers).

Finally, the protonated metabolites (**18**) and (**19**) undergo loss of 58 or 59 Da, i.e. loss of C_3H_6O or C_3H_6OH from the protonated molecule (fragmentation route C in Fig. 1) which unambiguously proves a hydoxylation of the isopropyl group. The observed loss of water and the $[A_2\text{-H}]^+$ ions confirm this assignment.

Table 1 shows the remaining hydroxylated metabolites (**20**)–(**23**) and their respective hydroxylation sites, which

were located by considering the further fragments of these metabolites. The exact sites of hydroxylation of ring B in (**21**) and (**23**), i.e. C_{15}, C_{16} or C_{19}, cannot be derived from the mass spectra. Although a confirmation of the hydroxylation sites by NMR was desirable, it was not possible for intensity reason.

3.1.6. Metabolites formed by oxidation of the methyl group bound to nitrogen

The metabolites (**24**) and (**25**) are of particular interest, as they are formed by oxidation of the methyl group bound to nitrogen. The quasi molecular ion of (**24**) at $m/z = 471$ is 16 Da higher than that of verapamil, which is consistent with a hydroxylation. As the m/z values of $[B_1]^+$ and $[B_3]^+$ are not shifted when compared to verapamil itself, hydroxylation must have occurred at the methyl group bound to nitrogen. The observed loss of water leading to m/z 453 is consistent with a hydroxylation. Thus, we conclude that a carbinolamine is formed as previously discussed by us in detail [8]. Finally, the metabolite (**25**) shows a $[M + H]^+$ ion at $m/z = 469$, consistent with the aldehyde structure shown in Table 1. This assignment is confirmed by the observed loss of 28 Da leading to a very abundant ion at $m/z = 441$. Although high resolution MS data are not available, the only reasonable explanation for this observed loss is elimination of CO (the isobaric loss of C_2H_4 is not observed with verapamil or any metabolite identified so far). This explanation is also consistent with the proposed aldehyde. The fragments at $m/z = 151$ and 165 further support this assignment. It is likely that (**24**) and (**25**) are intermediates of norverapamil (**2**), i.e. that the oxidation of the methyl group bound to nitrogen proceeds via (**24**) and (**25**) to (**2**).

In addition to verapamil, also 2, 3, 6, 15, 16, 19 verapamil-d_6 was incubated as described in Section 2. As only all aromatic hydrogens, and not the aliphatic and methoxy hydrogens mainly involved in the discussed biotransformation processes, were replaced by deuterium, the results from verapamil-d_6 are in agreement with the above conclusions (see Table 1, footnote f); however, they did not provide any additional proof for the structure assignment.

3.1.7. Phase II metabolites

Phase II metabolites were observed for 13 of the 24 identified metabolites and for verapamil itself. The collision-induced fragments are summarized in Table 1. The MS^2 spectra of the conjugates are (with one exception) dominated by an abundant loss of 176 Da, demonstrating a conjugation by glucuronic acid (176 Da = glucuronic acid – H_2O). Metabolite (**5**) showed an abundant loss of 162 Da, proving the conjugation with glucose (152 Da = glucose – H_2O). Apart from this dominating dissociation leading to the protonated phase I metabolite, the MS^2 spectra exhibited only few additional non-specific fragments, which provide no information on the exact site of glucuronidation or glucosidation (see Section 4).

4. Discussion

4.1. Mass spectrometry

The results demonstrate that, at least for verapamil and its metabolites, LC/MS in the MS^n-mode is well suited for an identification of metabolites in extracts of cell culture media. The collision-induced dissociation of the protonated molecules of verapamil and all 24 phase I metabolites is summarized in the general fragmentation schemes shown in Fig. 1. A collision-induced fragmentation leads to structure-specific ions formed by bond cleavages in the aliphatic moiety of the molecule (with and without hydrogen transfer). This fragmentation predominantly leads to thermochemically stable products, i.e. even-electron ions and neutral molecules (with the exception of the elimination of the isopropyl group which is predominantly lost as radical (see above and also Table 1)). The observed neutral losses (in particular water, ammonia, methylamine, carbonmonoxyde and acetone) provide valuable information for identifying structural features as demonstrated in Section 3.

In most instances, the structure of the phase I metabolites can be identified unambiguously with mass spectrometry. For instance, and as demonstrated in Section 3, it is possible to distinguish between a *O*-demethylation on ring A or B of verapamil, while mass spectrometry fails to distinguish between isomers due to a different substitution on one ring. This information is in principle available from NMR spectroscopy. However, if the biotransformation of a drug is studied in cell cultures, the concentrations of the metabolites are usually too low for NMR or LC/NMR measurements. Nevertheless, several verapamil metabolites in human urine have recently been identified by us using LC/NMR/MS. An extrapolation of these data to the metabolism in hepatocytes studied here has provided additional structure information. Thus, the *O*-demethylation in ring B involved the methoxy group in para position [9].

5. Phase I and phase II metabolites

Twenty-four phase I metabolites were identified, of which (**2**) (norverapamil), (**3**) (D-620), (**4**) (D-717), (**5**) (D-617), (**7**) (D-702), (**8**), (**10**), (**11**) and (**12**) (D-715) have been reported before. We recently reported the identification of metabolites (**24**) and (**25**) in cultures of primary cardiomyocytes [8]. Now, we report further novel phase I metabolites, including (**6**), (**9**), and (**13**)–(**23**). The metabolite (**6**) is generated by dealkylation, *O*- and *N*-demethylation, while (**9**), (**13**) and (**14**) represent other *O*-demethylation products; in fact, with (**13**) and (**14**) two successive *O*-dealkylations must have occurred as shown in Table 1. The metabolites (**15**)–(**23**) are formed by hydroxylation of verapamil or norverapamil as discussed in Section 3.

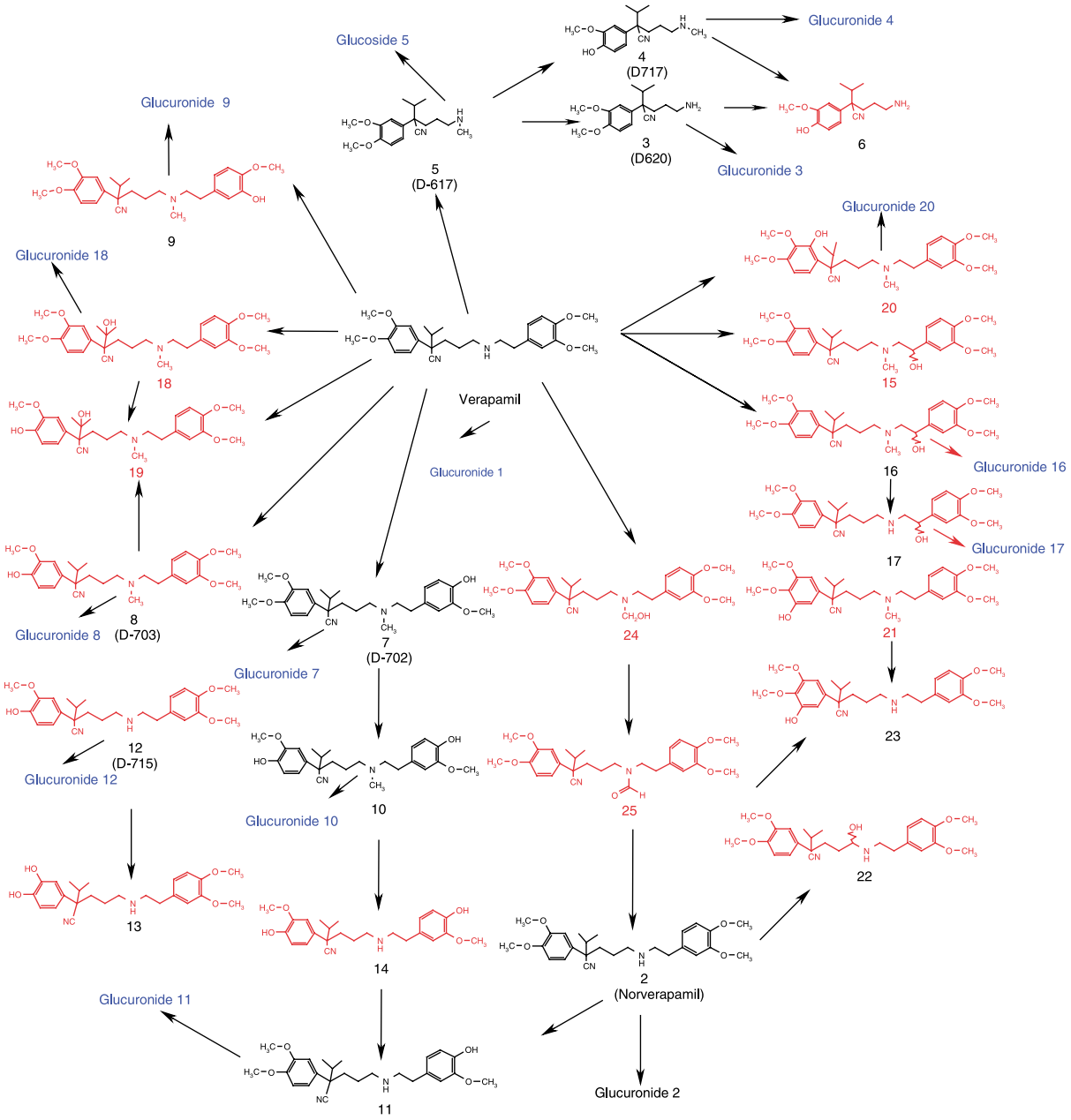

Fig. 2. Proposed structures for verapamil metabolites and metabolism pathway.

The singly or doubly demethylated or dealkylated metabolites (**2**)–(**5**), (**7**)–(**12**) are formed in the highest abundance (see Table 1).

The remaining metabolites (**6**) and (**13**)–(**25**), are only formed in minor amounts and are only detectable when at least a pool of 10 ml of cell culture supernatant was available, The estimated LOD for these metabolites is 1–5 pmol/ml using a sample size of at least 10 ml cell culture supernatant.

Hydroxylation of verapamil or norverapamil has not been described previously. As discussed above, hydroxylation occurs at almost any aliphatic carbon and in two instances at ring B.

All phase I metabolites are summarized in Fig. 2, which describes the most likely metabolic pathway of verapamil.

In addition, we report 14 phase II conjugates, of which the norverapamil glucuronide, i.e. (**2**) has previously been reported as an ester in GC–MS experiments [4]. The remaining 13 glucuronides are novel and are reported here for the first time.

If the phase I metabolite has no hydroxyl group, the glucuronides must be *N*-bound. This is the case for four phase II metabolites: one quaternary *N*-bound glucuronide (**1**), the norverapamil glucuronide (**2**), a secondary *N*-bound glucuronide (**3**) and one *N*-glucoside (**5**). If the phase I

metabolite has one or several hydroxyl groups and no primary or secondary amino functionality (i.e. if upon biotransformation the methyl group bound to nitrogen is retained), the glucuronide must be *O*-bound. This is the case for the seven glucuronides (**4**), (**7**)–(**10**), (**16**) and (**18**). However, if the phase I metabolite contains both a hydroxyl and a primary or secondary amino group (i.e. if the phase I metabolite is derived from norverapamil or formed by dealkylation), the glucuronide could be either *O*- or *N*-bound. This is the case for the glucuronides (**11**), (**12**) and (**17**). The glucuronide (**12**) has recently been found by us in human urine at relatively high concentrations, so that a LC/NMR measurement was possible [9]. The NMR data demonstrated unambiguously that the glucuronide (**12**) was *O*-bound. It is very likely that this result can be extrapolated to the glucuronide (**12**) formed in hepatocyte cultures as described in this study. The same reasoning suggests that also the glucuronides of (**11**) and (**17**) are *O*-bound.

Besides these conjugated metabolites, almost all metabolites also appear in their non-conjugated form. In addition, we identified eleven phase I metabolites, (**13**)–(**15**) and (**19**)–(**25**), which could not be detected as conjugates. However, this does not rule out that conjugates are also formed with these metabolites. As the ionization efficiency of the glucuronides under electrospray conditions is about 10 times lower than that of the phase I metabolites, these metabolites could probably not have been detected for sensitivity reasons.

The observation of the quaternary *N*-glucuronide of verapamil (**1**) and the *N*-glucoside of dealkylverapamil (**5**) is remarkable as *N*-glucosides and quaternary *N*-glucuronides are only rarely found [10–14].

In incubation assays with antipodes, we show that the *S*-enantiomer of verapamil is preferably metabolized. Glucuronides are also preferably formed by the *S*-enantiomer, indicating that the glucuronidation is also an enantioselective process with emphasis on the *S*-enantiomer in case of verapamil. The metabolite (**9**) was only detected after incubation with the *S*-form. As the abundance of this metabolite is low, the *R*-enantiomer could not be detected because of insufficient sensitivity. It is remarkable that metabolite (**23**) is preferably formed in its *R*-form.

Nelson et al. found for the metabolites (**3**) and (**4**) *S*/*R* ratios of 1.2 with rat liver microsomes and of 1.56 and 1.02 with human liver microsomes [2,15]. For metabolite (**5**), they found *S*/*R* ratios of 0.78 with rat liver microsomes and of 1.00 in human liver microsomes. It is noteworthy that the *S*/*R* ratios have not been determined for metabolites from cultured rat hepatocytes.

In conclusion, we report a total of 24 phase I and 14 phase II metabolites, of which 13 phase I and 13 phase II metabolites are novel. Our study provides new insight into the true complexity of verapamil's metabolism and demonstrates the power of LC–MS/MS in metabolism research.

Acknowledgements

The authors gratefully acknowledge Bruker-Daltonik (Bremen, Germany) for loaning the Esquire-LC and Prof. W.L. Nelson (University of Washington, Seattle) for providing the D-715 metabolite and verapamil-d_6.

References

[1] M. Eichelbaum, M. Ende, G. Remberg, M. Schomerus, H.J. Dengler, Drug Metab. Dispos. 7 (1979) 145.
[2] W.L. Nelson, L.D. Olsen, D.B. Breitner, R.J. Pallow Jr., Drug Metab. Dispos. 16 (1987) 184.
[3] W.L. Nelson, L.D. Olsen, Drug Metab. Dispos. 16 (1988) 834.
[4] A.E. Mutlib, W.L. Nelson, J. Pharm. Exp. Ther. 252 (1990) 539.
[5] O. Richter, M. Eichelbaum, F. Schöneberger, U. Hofmann, J. Chromatogr. B. 738 (2000) 137.
[6] P.O. Seglen, J. Toxicol. Environ. Health 5 (1979) 551.
[7] J.C. Dunn, M.L. Yarmush, H.G. Koebe, R.G. Tompkins, FASEB J. 3 (1989) 174.
[8] M. Walles, T. Thum, K. Levsen, J. Borlak, Drug. Metab. Dispos. 29 (2001) 761.
[9] J. Borlak, M. Walles, M. Elend, T. Thum, A. Preiss, K. Levsen, Xenobiotica 33 (2003) 655.
[10] S.H.L. Chiu, S.E.W. Huskey, Drug Metab. Dispos. 26 (1998) 838.
[11] M.L. Dahl-Puustinen, L. Bertilsson, Pharm. Toxicol. 61 (1987) 342.
[12] P.V. Macrae, M. Kinns, F.S. Pullen, M.H Tarbit, Drug Metab. Dispos. 18 (1990) 1100.
[13] S.K. Kirkman, M.Y. Zhang, P.M. Horwatt, J.A. Scatina, Drug Metab. Dispos. 26 (1998) 720.
[14] B.K. Tang, B. Yilmaz, W. Kalow, Biomed. Mass. Spectrom. 11 (1984) 462.
[15] W.L. Nelson, L.D. Olsen, D.B. Breitner, R.J. Pallow Jr., Drug Metab. Dispos. 16 (1988) 834.